Comparing Two Electrospinning Methods in Producing Polyacrylonitrile Nanofibrous Tubular Structures with Enhanced Properties

Habeeb, Salih Abbas; Rajabia, Laleh*[+]

Polymer Research Lab., Faculty of Petroleum and Chemical Engineering, Razi University, Kermanshah, I.R. IRAN

Dabirian, Farzad

Department of Textile Engineering, College of Engineering, Razi University, Kermanshah, I.R. IRAN

ABSTRACT: *Polyacrylonitrile nanofibrous tubular structures were produced through typical and opposite charge electrospinning methods and the effect of the method as well as the two key electrospinning parameters, namely concentration of the electrospinning polymer solution and rotational speed of mandrel collector on properties of such tubular structures were studied. The smples were characterized by X-ray diffraction, scanning electron microscopy, Fast Fourier Transform method and tensile tests. Increasing polymer solution concentration considerably increased the diameter of the nanofibers and decreased the bead formation, where the increasing ranges of the average diameters were larger and sizes of beads were smaller for the nanofibers produced by the opposite charge set-up. Nanofibers' diameter, on the other hand, decreased as the speed of the rotational mandrel increased and the observed decline was greater in the opposite charge method, especially at higher concentrations of polymer solution. An inversion point for the anisotropy of mechanical properties was found to be around 2164 rpm. The aspect ratio of the nanofibers also increased with increasing the take-up speed. Increasing the take-up speed increased the mechanical force of pulling the jet, resulting nanofibers with smaller diameter, which in turn improved the crystallinity and molecular orientation of the fibers that explained the enhanced tensile properties for smaller diameter fibers. Different breaking mechanisms for the randomly oriented fibers and directionally aligned nanofibers were observed.*

KEYWORDS: *Opposite charge electrospinning; Tubular structure; Nanofiber diameter; Alignment; Crystalline properties; Tensile properties.*

INTRODUCTION

Electrospinning has been the most successful method of producing nanofibers using electrical charges [1]. The advantages of this method are that it is relatively easy, low-cost, high-speed with vast materials selection,

** To whom correspondence should be addressed.*
+ E-mail: laleh.rajabii@gmail.com
1021-9986/2019/3/23-42 *20/$/7.00*

and versatility. Furthermore, the technique allows control over fiber diameter, microstructure, and arrangement [2, 3]. Electrospun nanofibres from different polymers have been used in filters, composites [4], tissue engineering scaffold, protective clothing, electronics, catalysis, ceramic fibers, wound dressing, drug delivery materials and other applications [5]. The properties classify the applications of the nanofibers, for example, reduction in a dimension of nano fibers can lead to new properties, such as quantum effects, adsorption behavior, or catalytic selectivity [6, 7]. To fabricate fibers that are not only non-woven meshes but also aligned, patterned, twisted yarn, and three-dimensional structures, developing new methods for controlling the deposition behavior of the fibers either by mandrel collector shaft, rotating drums, disk collectors or parallel electrodes are required [5, 6] *Xie J.* and *coworkers* used the opposite charge nozzle's to align 3-D nanofibers into a uniaxial array [8]. They modified the typical set-up by installing two needles in opposite directions and pumping the polymer solution into needles by two syringe liquid pumps with the same injection rate. Aligned and molecularly oriented polyacrylonitrile nanofibers were also prepared using a non-conventional approach, that is using two needles in opposite positions and a rotating collector perpendicular to needle axis [9]. Electrospinning parameters can be classified into process parameters, solution parameters and ambient parameters [10, 11]. The concentration of polymeric solution plays an important role in the bounded properties of the electrospun nanofibers [12]. Highly concentrated solutions allow producing more uniform fibers with fewer beads and also production of larger fiber diameters [13-19]. The shape of the beads also changes from spherical to spindle like when the polymer concentration increases. On the other hand, the increase of polymer concentration plays an important role for alignment of nanfibers [20], which in turn affects the mechanical properties [21]. The electrospinning parameters such as polymer concentration, applied voltage and flow rate of solution strongly affect the solidification rate of the resulting nanofibers and the fast stretching and solidification of the polymer chains lead to another important effect which is decreasing crystallinity of polymer nanfibers since the stretched chains do not have enough time for crystal formation. However, these non-crystalline polymer chains in the nanofibers are yet strongly oriented [13]. Recent studies have shown that alignment of nanofibers improved molecular orientation and, as a consequence, improved mechanical properties than the randomly oriented nanofibers [22, 23]. Studying the electrospun nanofibers produced at different rotational speeds indicated that the rotating speed had an important effect on their tensile properties [24]. *Kenawy E.R.* and his coworkers showed that, as the rotational speed increased, the breaking strength and the initial module were enhanced due to increaseing crystallinity [24] and varying rotational speed was shown to lead to changes in the material mechanical anisotropy index as well [25]. *Ipek Y. Enis* and coworkers produced single layer vascular grafts by a custom designed electrospinning apparatus [26]. The authors reported that the fiber orientation was imroved with increased rotational speed and also polymer type and the rotational speed of the collector significantly influenced ultimate tensile strength and elongation at break values of scaffolds tested in the radial direction. In another work, *Enis* and coworkers reported on both single layer and bilayer tubular scaffolds with inner diameter of 6 mm which were electrospun from different molecular weights polycaprolactone and poly (L-lactide) caprolactone polymers. Their results indicated that the use of different biodegradable polymers in different combinations in each layer caused notable differences in fiber morphology and mechanical performance of the scaffolds [27].

This work reports on the production and characterization of PAN nanofibrous tubular structures obtained through both typical and opposite charge electrospinning methods to compare the effect of the method as well as the two key electrospinning parameters, namely concentration of the electrospinning polymer solution and rotational speed of mandrel collector on properties such as nanofiber diameter and alignment, crystalline and tensile properties of the tubular structures. The production of such nanostructures (tubular) through opposite charge electrospinning method with the type of collector used in the current work has not been reported so far. Thus, attempts were made to fabricate nanofibrous tubular structures by the more efficient electrospinning method (opposite charge method). Moreover, the present work reports on structures, showing anisotropic properties, claiming the production of tubular nanostructures with decreased nanofibers diameter

(improved aspect ratio) with uniform thickness and enhanced alignment and tensile properties via combinational controlling of collector shape and collector rotation.

EXPERIMENTAL SECTION

Materials and Methods

Commercial Polyacrylonitrile (PAN) powder with a molecular weight of 100,000 (g/mol) was supplied by Poly Acryl Company, Iran and Dimethyl formaldehyde (DMF) was obtained from Merck (Schuchardt OHG 85662 Hchenbrunn, Germany). The schematic diagram of the typical and opposite charge electrospinning methods used are shown in Fig. 1.

Preparation of the Electrospinning Polymeric Solutions

The appropriate amounts of PAN and DMF were mixed using a heating magnetic stirrer at the temperature of 40 ºC for 4hr to obtain a well-dissolved transparent light yellow homogeneous polymer solution, ready for electrospinning by two set-ups to produce the corresponding nanofibrous tubular structures as shown in Fig. 1. Table 1 presents the electrospinning conditions.

Production Steps of the Nanofibrous Tubular Structures

The nanofibrous tubular structures were produced through the following steps:

A 0.25mm copper wire was wrapped around a 3 mm diameter stainless steel rod. The assembly was immersed in a concentrated glucose solution and then dried for 20 minutes in the air. The dried assembly was used as the rotating mandrel in both the electrospinning set-ups for the production of the nanofibrous tubular structures. The whole above mentioned assembly was then immersed in distilled boiling water as a result of which the metal rod was easily removed. Then the copper wire with the electrospun nanofibers around it was dry for 15 min in an air oven at the temperature of 50-60 °C under atmospheric pressure. At last, the wire was straightened by pulling from both ends and removed easily. The inner diameter of each tube was 3.5 mm.

Instruments

The structural and morphological characterization of the polymeric structures were performed by X-ray diffraction (XRD), [Philips PAN alytical: X'Pert Pro MPD X-ray diffractometer at room temperature, using X-Ray Tube: Cu (Kα= 1.54 Å), Generator Settings: 40 mA, at 40 kV and 2θ = 3º-40º, Step Size (°2Th.): 0.0260.]; Scanning electron microscopy (SEM), [KYKY–EM 3200 model, the surface of samples was coated with a layer of gold with a thickness of 100 Å by using the sputter coater KYKY-SBC12]. The average diameter with standard deviation (Stdev) and beads size was calculated using the Digitizer image analysis software program and the Frequency histograms of nanofibers diameter distribution were plotted by QI Macros (SPC Software for Excel, Six Sigma Software). Fast Fourier Transform (FFT) method was used to identify the functional groups and vibrational modes of the materials as well as to quantify the alignment of nanofibers. Digitized SEM images were converted to 8-bit grayscale TIF files and changed to (960 x 960) pixels and the images were processed with Image J software (NIH, http://rsb.info.nih.gov/ij) supported by an oval profile plugin (authored by Bill O'Connell) and also, the Fourier Painter-2D Fourier Transforms, image analysis software by J Crystall Soft, 2015 was used to analyze the FFT results. The original SEM image information converted from the real space into the mathematical frequency space through FFT function. Fiber alignment was analyzed using the image-processing technique by Fourier Power Spectrum Method (FPSM). This method has been used to evaluate the orientation of the fibers with Matlab program, which was used to calculate the Angular Power Spectrum (APS). Tensile properties of the nanofibrous tubular structures were obtained by the Universal Testing Machine (UTM), [Hi-Zwick model 1446-60, the samples were prepared according to the ASTM D-638-14 standard (2.0 cm in length, mounted on the clamps to be tested at the speed of 5 mm/min until the sample broke).

RESULTS AND DISCUSSION

Effect of the Electrospinning Parameters on Nanofiber's Diameter in the nanofibrous tubular structure

To study the effect of concentration, other electrospinning parameters (Table 1) were kept constant, whereas, the concentration of the PAN solution varied from 9 to 17 wt. % to study its presence in various amounts on the fabricated nanofiber's diameter. Fig. 2 shows the average nanofiber diameters against various

Table 1: The electrospinning conditions.

Typical electrospinning set-up		Opposite charge electrospinning set-up	
Parameters	Process conditions	Parameters	Process conditions
C (wt.%)	-	C (wt.%)	-
9	1- d = 20 cm	9	1- d = 15 cm
11	2- S = 0.5 mL/h	11	2- D = 11-13 cm
13	3- R = 4328 r p m	13	3- S = 0.5 ml / hr.
15	4- A = 20 kV	15	4- R = 4328 r p m
17	-	-	5- A = 20 kV
R (r p m)	1- d = 15 cm	R (r p m)	1- d = 20 cm
1515	2- S = 0.5 mL/h	1515	2- D = 11-13 cm
2164	3- C = 15 wt.%	2164	3- S = 0.5 ml / hr.
4328	4- A = 20 k V	4328	4- C = 15 wt.%
6492	-	6492	5- A = 20 kV

d = distance between needle and collector (cm) , S= Solution feed rate (mL/hr.), R= Rotational speed (r pm) , A= Applied voltage (kV) , D= Distance between two needles (cm) , Co= Concentration of PAN / DMF (wt.%)

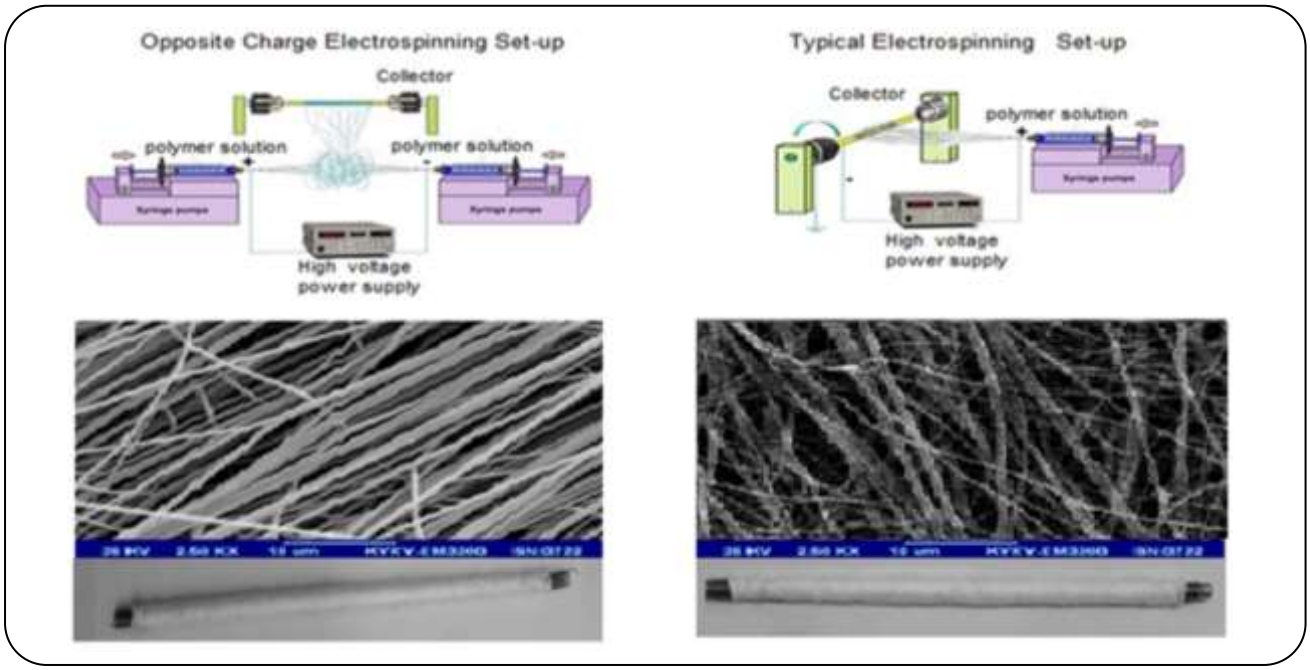

Fig. 1: The schematic diagram of the typical (left) and opposite charge (right) electrospinning set-ups (operated at 1515, 2164, 4328 and 6492 rpm as the mandrel rotational speed) to produce nanofibrous tubular structures.

concentrations of PAN produced by two different electrospinning methods.

The obtained results (Fig. 2) reveal that as the concentration of PAN increased from 9 to 17 wt.%, the average diameters with standard deviation (stdev) and diameter ranges of the electrospun PAN nanofibers produced by typical set-up increased from 171.4±36.6 nm to 907.6±156.6 nm and from 99-270 nm to 652-1264 nm respectively. The same increasing trend was observed for the nanofibers produced by the opposite charge set-up, where on increasing the concentration of the PAN solution from 9 to 15 wt.%, the average diameters with

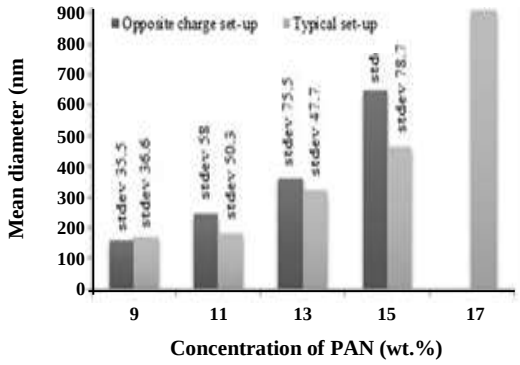

Fig. 2: Effect of concentration of PAN on the average nanofiber's diametesr produced by typical and opposite charge electrospinning methods.

standard deviation (stdev) and diameter ranges increased from 159.5±35.6 to 649.8±117.1nm and from 106-251 to 429-851 nm, respectively. The solidification rate of polymer solution varies with the electrospinning parameters such as polymer concentration. Thus, increasing the electrospinning solution concentration produces fibers with larger diameters [13]. The increasing range of the average diameters with standard deviation (stdev) and a diameter range of the electrospun PAN nanofibers was higher for the nanofibers produced by the opposite charge set-up, where, the mechanical force was perpendicular to the electrical force and the effect of the net force for stretching nanofibers was less than that of the typical set-up. It is known that the fiber length is a function of the stability of the spinning process and can be many hundreds of meters. It is also believed that, the fiber diameter, conversely, is dependent on a large number of interdependent spinning parameters including the average polymer chain length, the concentration of polymer in solvent, the distance between nozzle and collector, the electric field strength and shape, the flow rate of the solution through the nozzle, and the electromechanical properties of the solution [23, 28]. The length-to-diameter ratio (aspect ratio) decreased on increasing the PAN solution concentration and the solution with lowest PAN concentration was stably electrospun. The nanofibers' diameters distribution became gradually broader with increasing the concentration of PAN electrospinning solution for both typical and opposite set-ups. Increasing the nanofibers' diameters was due to expansion of the nanofibers diameter distribution and decreasing the specific surface area. Fiber formation is a function of the polymer concentration where an optimal range of concentration increases the chances of polymer chain entanglement, resisting bending and thus, resulting in fine fibers. The higher solution viscosity limits solvent evaporation and necking, resulting thicker fibers. Fig. 3 presents the SEM micrographs of the nanofibers produced from varrying PAN solution concentrations through the typical and opposite charge electrospinning methods. Not only does the SEM produce topographical information as optical microscopes do, it also provides the chemical composition information near the surface [29]. The SEM micrographs (Fig. 3) illustrate the effect of polymer solution concentration on bead formation of the nanofibers fabricated through two different electrospinning methods. As the concentration of PAN electrospinning solution increased, the diameter of the fiber increased and fewer beads were formed along the length of the nanofibers (more uniform fibers formed), where the average distance between beads was longer and also the bead shapes were changed from spherical to spindle-like.

Fig. 3 also shows that, the number and size of the beads produced at a higher concentration by the opposite charge set-up were fewer as well as smaller than those produced by typical set-up. Thus, the higher electrical force between the tips of the needles at the opposite charge electrospinning set-up was positively an affecting factor in this process. The best performing PAN electrospinning solution concentration was 15 wt.% among the four solutions studied by both the typical and opposite charge electrospinning set-ups. The polymer solution with 17 wt.% concentration was highly viscose, making the electrospinning process difficult and very time consuming. Thus it was subjected to electrospinning by the typical method, it was decided not to proceed with the other metod for this solution concentration.

A rotating stainless-steel mandrel with an inner diameter of 3.0 mm was used in this study as explained in the experimental section and the electrospinning conditions were as given in Table 1. To study the effect of rotating mandrel collector speed, the concentration of PAN solution was kept constant as 15wt % and nanofibers were produced through both, typical and opposite charge methods at four different take-up speeds as 1515, 2164, 4328 and 6492 rpm. Fig. 4 compares the average nanofiber diameters obtained from the 15 wt.% polymer

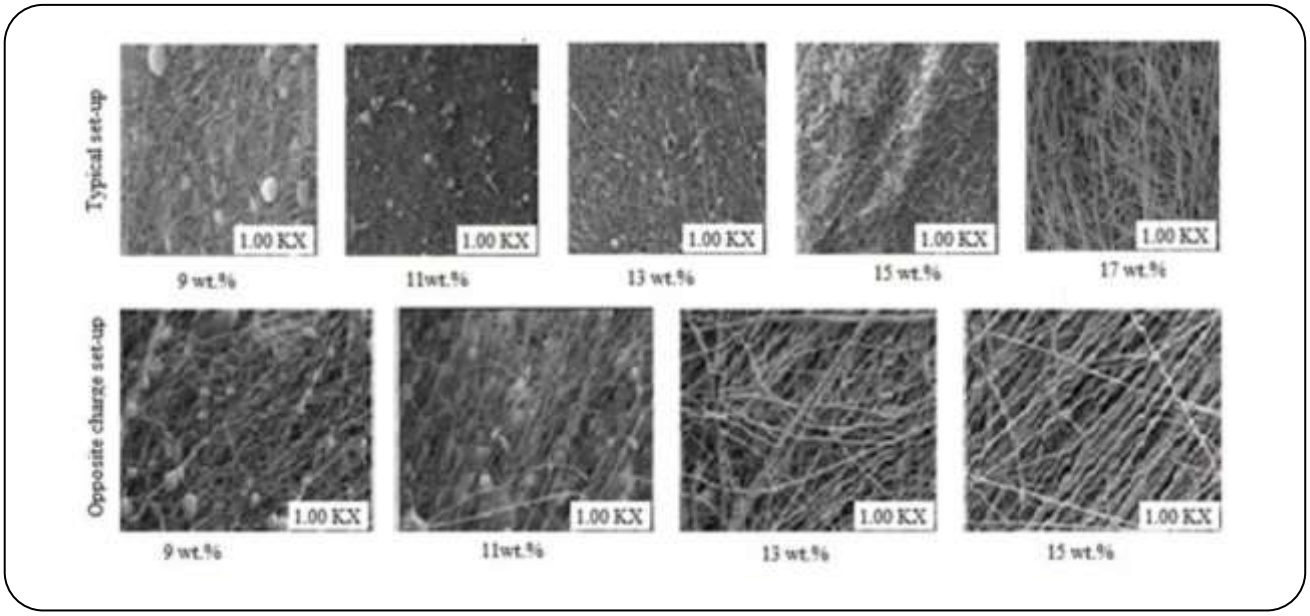

Fig. 3: SEM micrographs of the nanofibers produced from varying PAN solution concentrations through the typical and opposite charge electrospinning methods with the applied voltage of 20 kV and at the mandrel rotating speed of 4328 rpm.

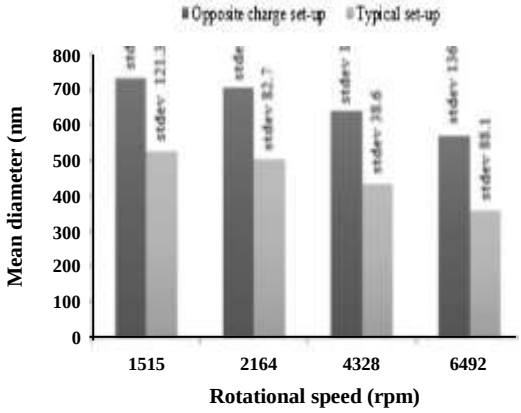

Fig. 4: Average nanofiber diameter obtained from the 15 wt.% polymer solution as a function of mandrel collector rotational speed produced from the typical and opposite charge electrospinning methods.

the solution as a function of mandrel collector rotational speed produced from the typical and opposite charge electrospinning methods.

The results revealed that, as the speed of the rotational mandrel increased from 1515 to 6492 rpm , the average diameter and the diameter range of the nanofibers decreased [(526.2 ±121.3 to 357.8 ± 88.1) nm (253–800 to 239–622) nm], [(730.1±138.3 to 569.1±136) (548-953 to 262–865) nm] for typical and opposite charge set-ups respectively and the nanofibers diameter distribution became gradually narrower with the increased speed of the rotating mandrel (Figs. 5 and 6). As the rotational speed increased, the imposed pulling force on nanofibers also increased. However, the net pulling force of the opposite set-up was less than that of the typical setup and thus, the observed decline in the average diameter and the diameter range of the nanofibers were greater than those obtained for the typical set-up, especially at a polymer concentration as high as 15 wt.%.

Effect of the Electrospinning Parameters on Alignment of Nanofibrous tubular structure

Fast Fourier Transform (FFT) method was used to examine the alignment of nanofibers, which calculates the Angular Power Spectrum (APS) and A(θ) to provide information on directionality of the texture through the following equation:

$$A(\theta) = \sum_{r-1}^{R} Pr(\theta) \quad (1)$$

Where P is a two-dimensional power spectrum for an N × N image picture, and r (varied from 1 to R) and (θ) (varied from 0 to π) are the variables in the polar coordinate system. R is typically chosen as N/2. The two-dimensional power spectrum function P(u, v) was calculated as follows: $P(u, v) = | F(u,v) |^2$ for u, v = 0, 1, 2, . , N-1, here F(u, v) are two-dimensional Fourier

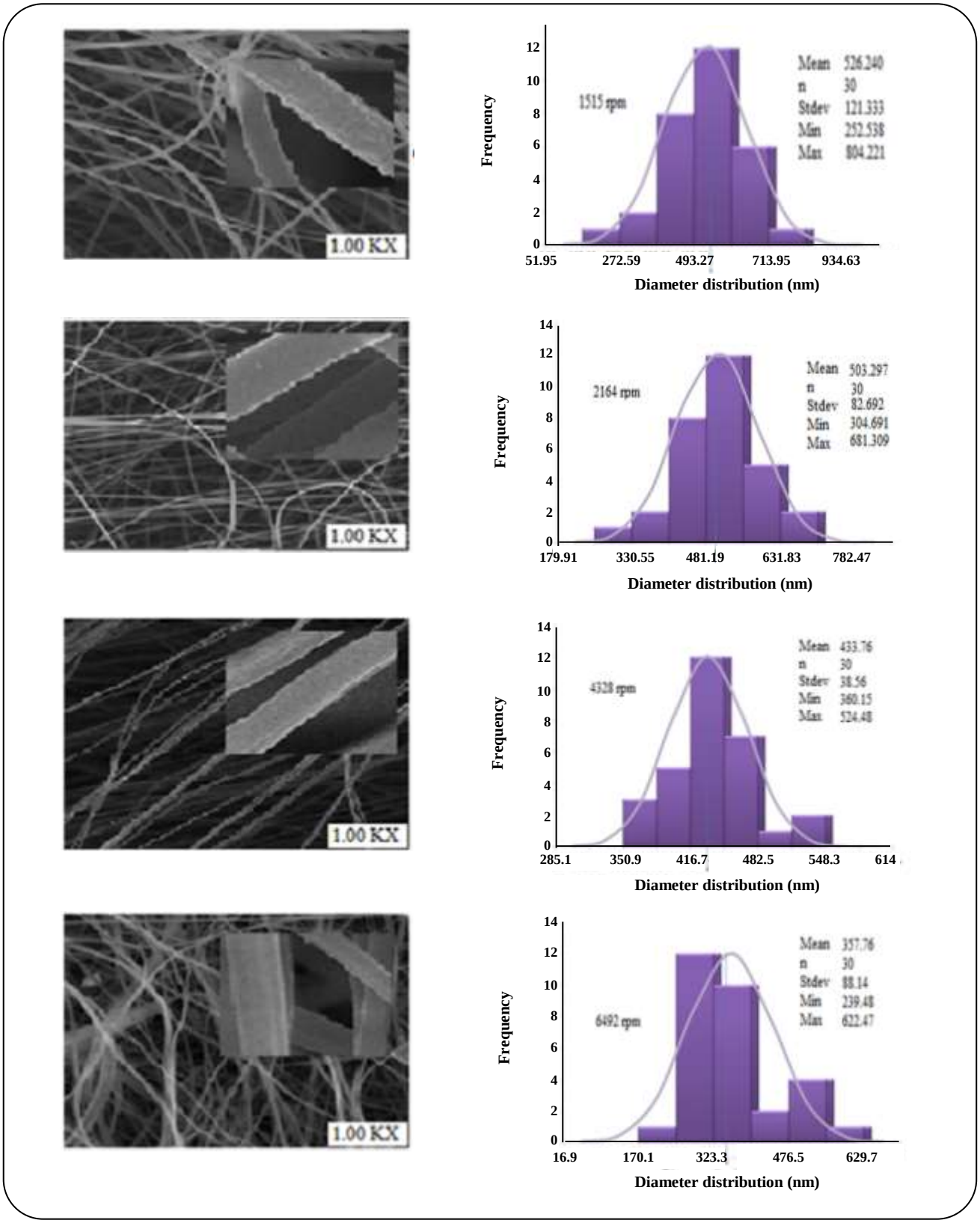

Fig. 5: Frequency histograms of nanofibers diameter distribution produced from the 15 wt.% PAN solution at four rotating mandrel speeds performed by the typical set-up.

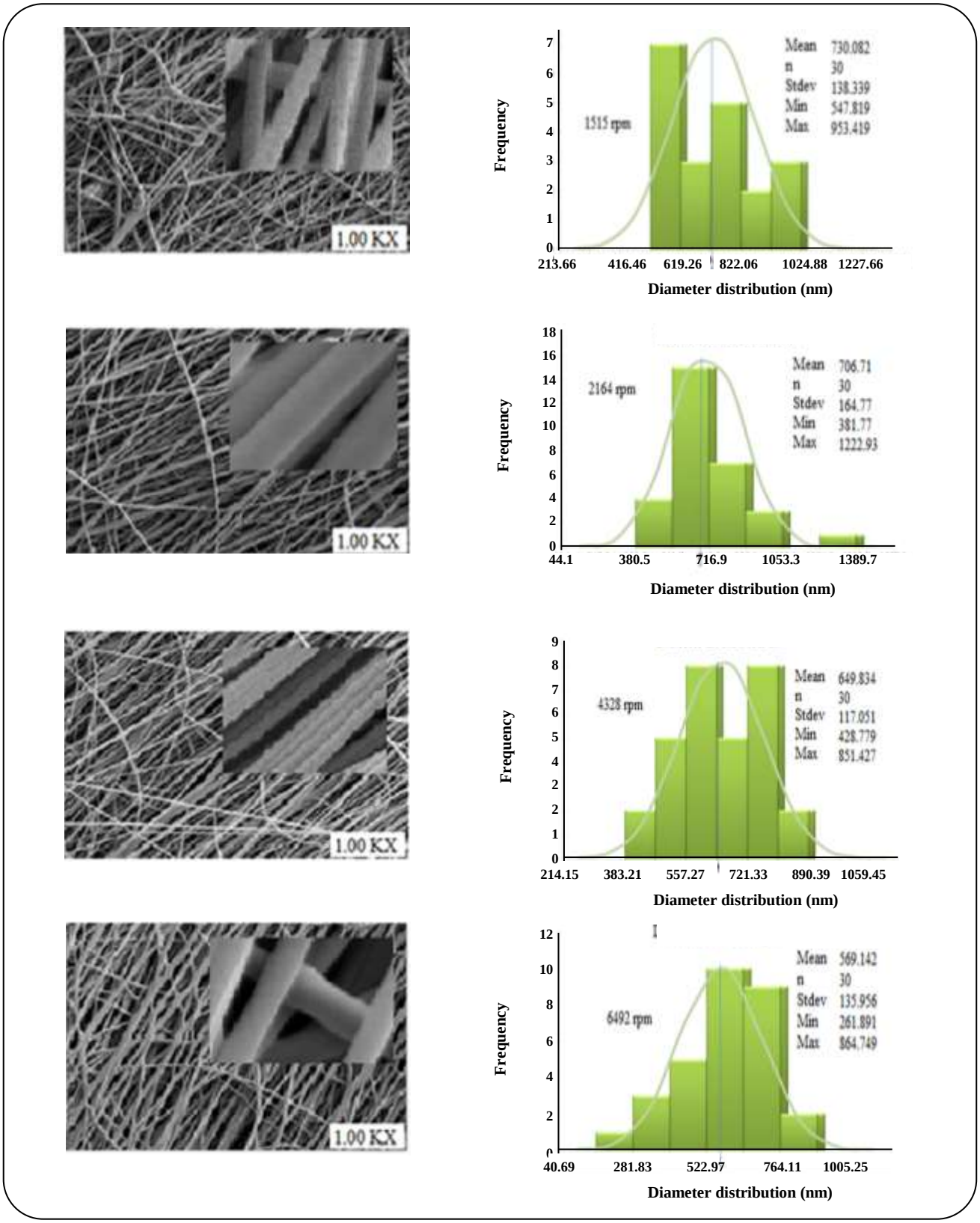

Fig. 6: Frequency histogram of nanofibers diameter distribution produced from the 15 wt.% PAN solution at four rotating mandrel speeds performed by the opposite charge set-up.

transforms of the image [30]. The original SEM image information converts from the real space into the mathematical frequency space through FFT function [31]. It has been reported that mandrel rotation speed should exceed 1000 rpm before expecting any change in fiber alignment [32]. The alignments are confirmed by converting the image by a Fast Fourier Transform (FFT) so as to observe the relative spatial dimensions between fibers in the form of brightness transitions. In electrospinning, the jet is traveling at a very high speed. A rotating collector will provide the solvent more chances to evaporate and thus, may increase the rate of evaporation of the solvent on the fibers. In order to align the fibers around the mandrel, it is necessary that the mandrel rotates at a very high speed so that the fibers can be taken up on the surface of mandrel and wounded around it. This will improve the morphology of the fiber where, distinct fibers are required. To proceed with the study of the effect of one parameter at a time on the corresponding property, the electrospinning conditions were kept constant (Table 1), whereas, the concentration of the PAN solution varied from 9 to 17 wt% to study its variation effects on the alignment of the fabricated nanofibers. As the concentration of PAN solution increased from 9 to 17wt % and from 9 to 15 wt.% to produce nanofibers by using typical and opposite charge electrospinning set-ups, respectively, the obtained nanofibers became more aligned. The solidification rate varied with the polymer concentration, electrostatic field, and gap distance, leading to another important effect, the retardation of the crystallization process as the stretched chains did not have enough time for crystal formation. Researchers have reported on highly oriented nanofibers, despite the polymer chain non-crystallinity at high concentrations [13, 14]. The degree of alignment was higher when opposite set-up was used to produce nanofibers than that of the nanofibers produced by the typical set-up, since the electrical force between two needles was higher and the distance was shorter (11-13 cm) for the former, while the distance between the needle and mandrel collector at typical setup was longer (15cm).

Figs. 7 and 8 show the Fast Fourier Transfer (FFT) approach of measuring the alignment rates of the nanofibers as well as the Fourier Painter-2D Fourier Transform. The FFT analysis of the SEM images of the nanofiber samples were used to characterize the anisotropy of the scaffolds to digitize the alignment level of the nanofibers. Patterned, grayscale pixels were distributed in the output image of the FFT analysis to reflect the degree of fiber alignment of the original data image [33]. Fig. 7 displays a significant difference between the FFT images of the aligned nanofibers and randomly-oriented nano fibers. The representative FFT of the original data image of the random fibers at the polymer solution concentrations of 9, 11 and 13 wt.% at typical method, generated an output image with symmetrically and circularly distributed pixels. On the other hand, the FFT data of the image with aligned fibers resulted in an output image with non-randomly and elliptically distributed pixels for the 15 and 17 wt.% produced nanofibers. The pixel intensities were plotted between 0 to 360°, and the degree of alignment in the FFT data reflected the shape and height of the peak. Also the higher the intensity and fewer occurrences of peaks indicated that the alignment of the nanofibers was highly ordered as presented in Fig. 8 for the nanofibers produced by the opposite charge method especially for the ones obtained from 15 wt.% solution concentration.

The obtained results revealed that the nanofibers produced from the 15 wt.% polymer solution fabricated through both, typical and opposite charge methods, had the best degree of alignment.

To study the effect of rotating mandrel collector speed on alignment, the concentration of PAN solution was kept constant as 15wt.% and nanofibers were produced through both, the typical and opposite charge methods with the rotational speed of the mandrel collector varying from 1515 to 2164 to 4328 and finally to 6492 rpm, keeping other electrospinning parameters constant. Some preferred diagonal alignments were detected at the rotating mandrel speed of 1515 rpm.

Fig. 9 and 10 show the SEM images and the FFT alignment histograms of the nanofibers produced from the 15 wt.% polymer solution fabricated through the typical and opposite charge electrospinning methods at four take-up speeds.

Increasing the take-up speed from 1515 to 6492 rpm, improving the alignment of the resulting nanfibers and also that, the FFT alignment variation values were higher when the opposite charge set-up was used, since the electrical force between two needles in the opposite charge set-up was higher than the electrical force between

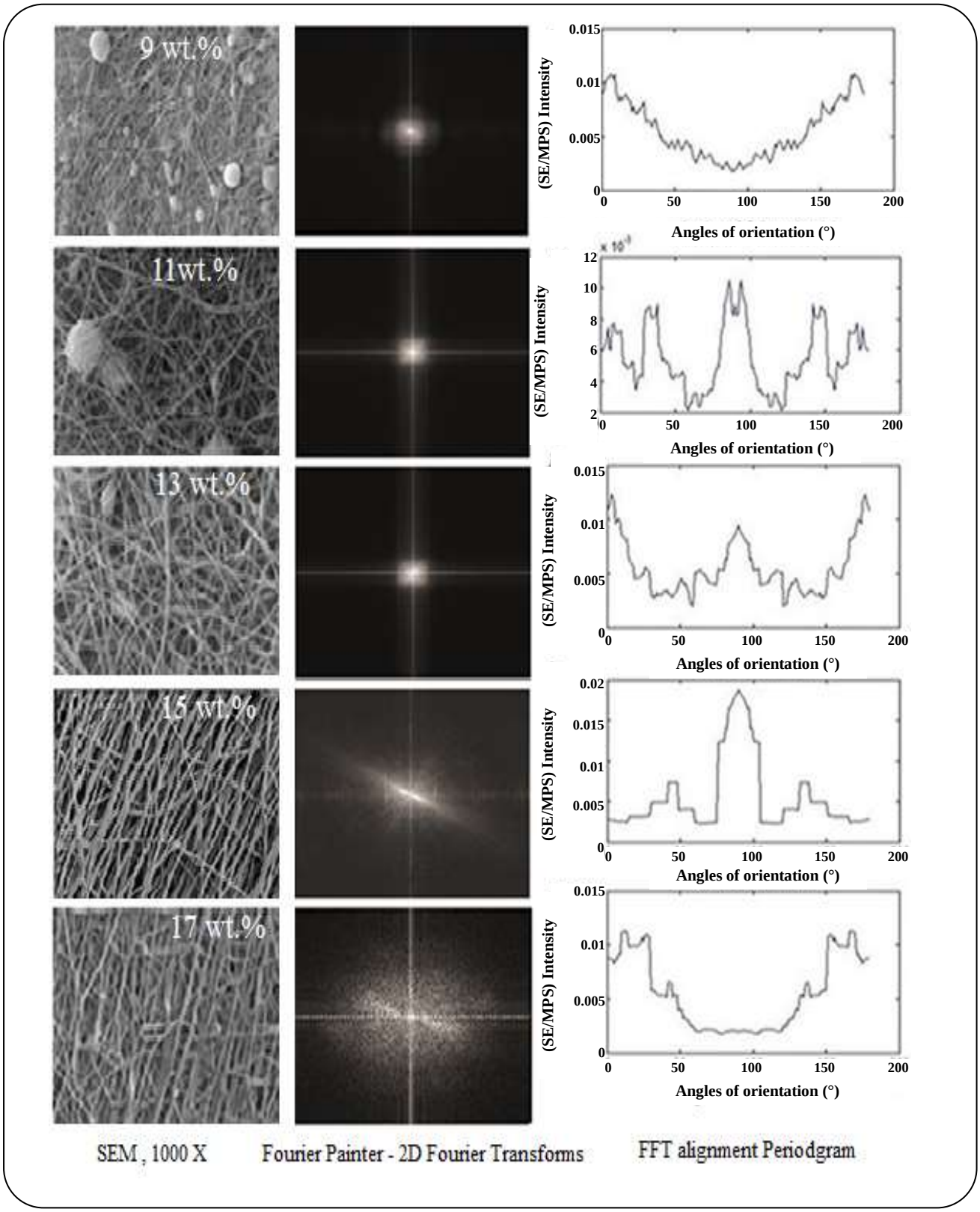

Fig. 7: SEM micrographs, Fourier Painter-2D Fourier Transforms Images and the FFT alignment Periodgram of the nanofibers produced from the polymer solutions with different concentrations obtained through typical electrospinning method with the rotating mandrel speed of 4328 rpm.

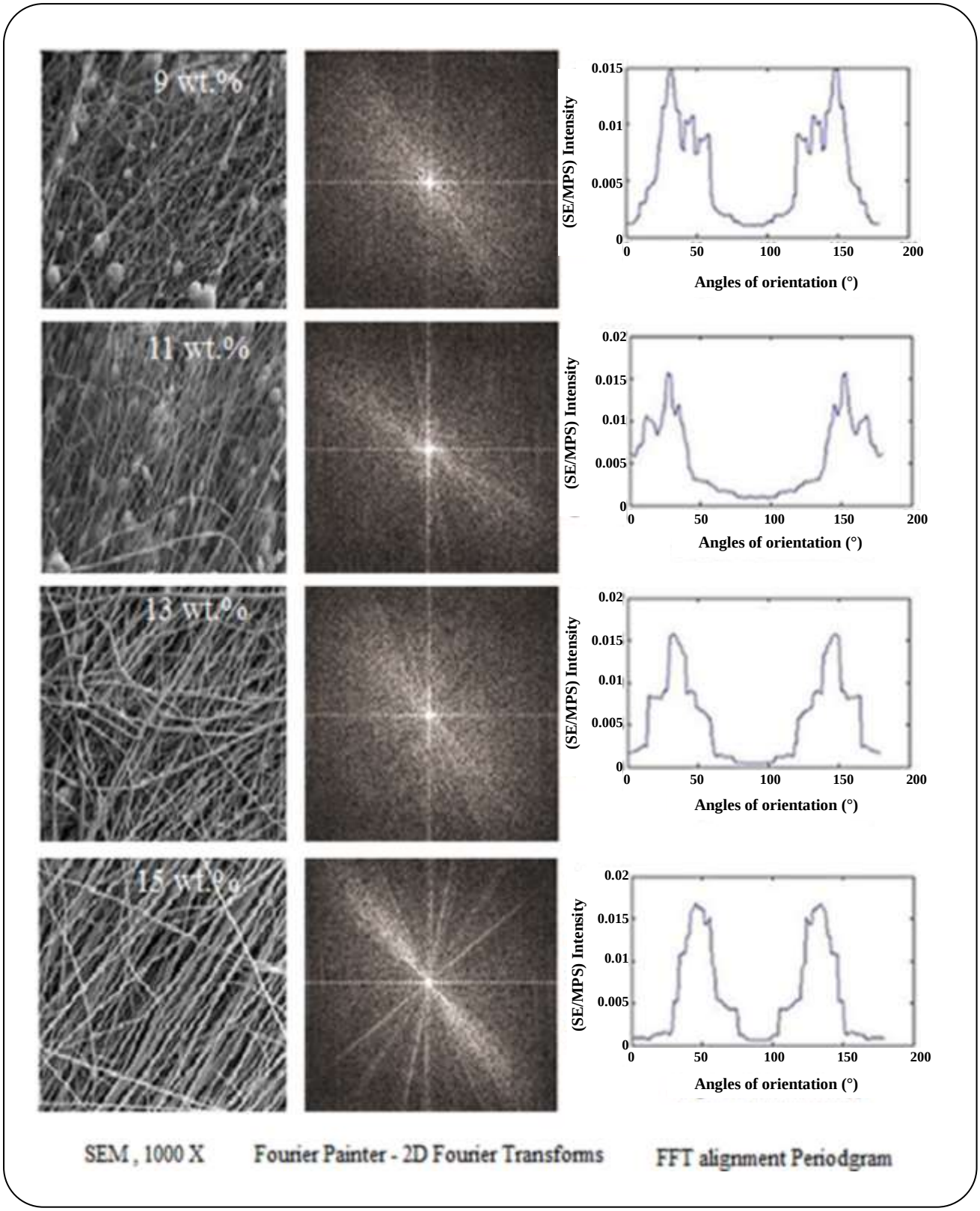

Fig. 8: SEM micrographs, Fourier Painter-2D Fourier Transforms Images and the FFT alignment Periodgram of the nanofibers produced from the polymer solutions with different concentrations obtained through opposite charge electrospinning method with the rotating mandrel speed of 4328 rpm.

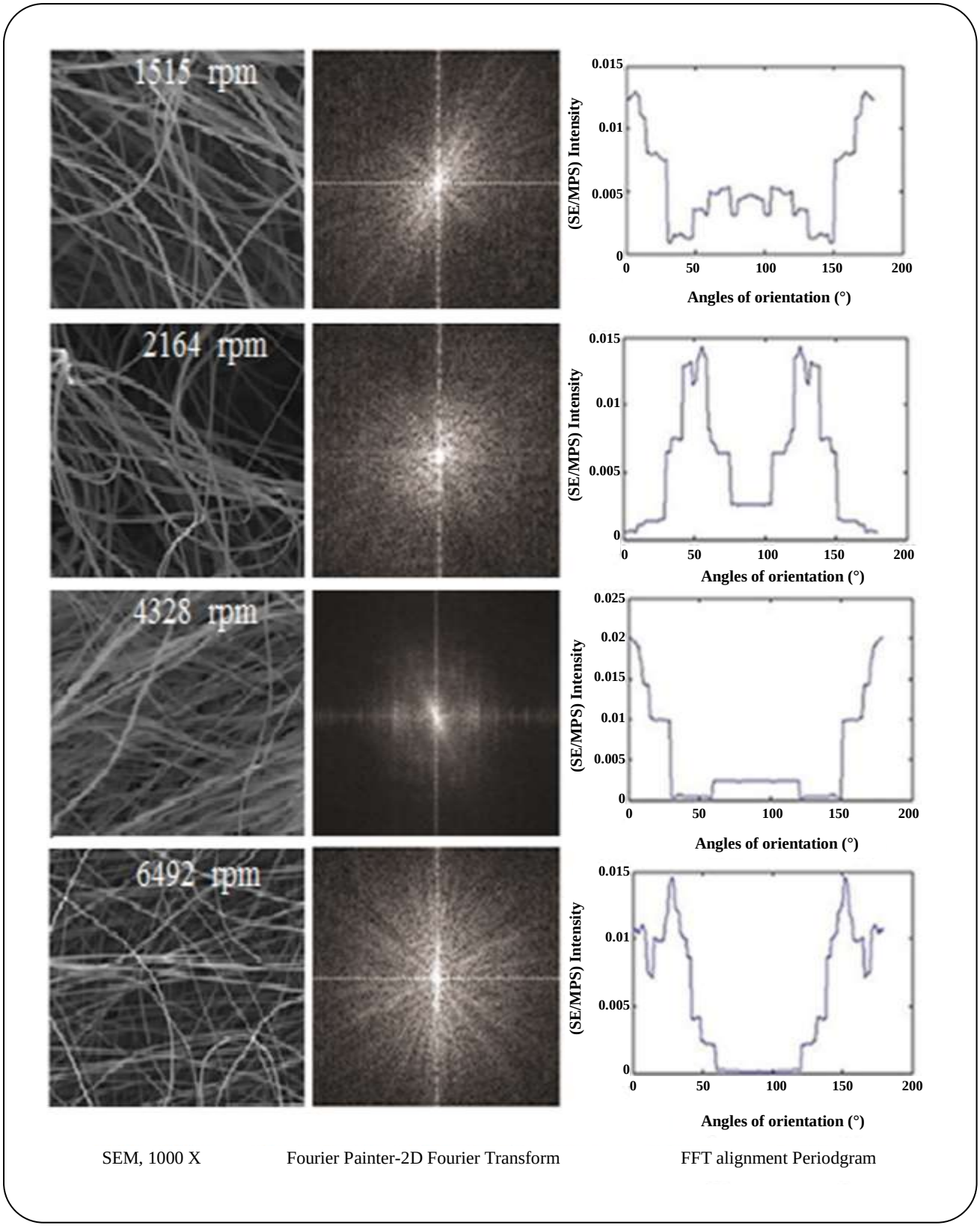

Fig. 9: SEM micrographs, Fourier Painter-2D Fourier Transforms images and the FFT alignment Periodgram of the nanofibers produced from the 15 wt.% polymer solution at four take-up speeds fabricated through typical electrospinning method.

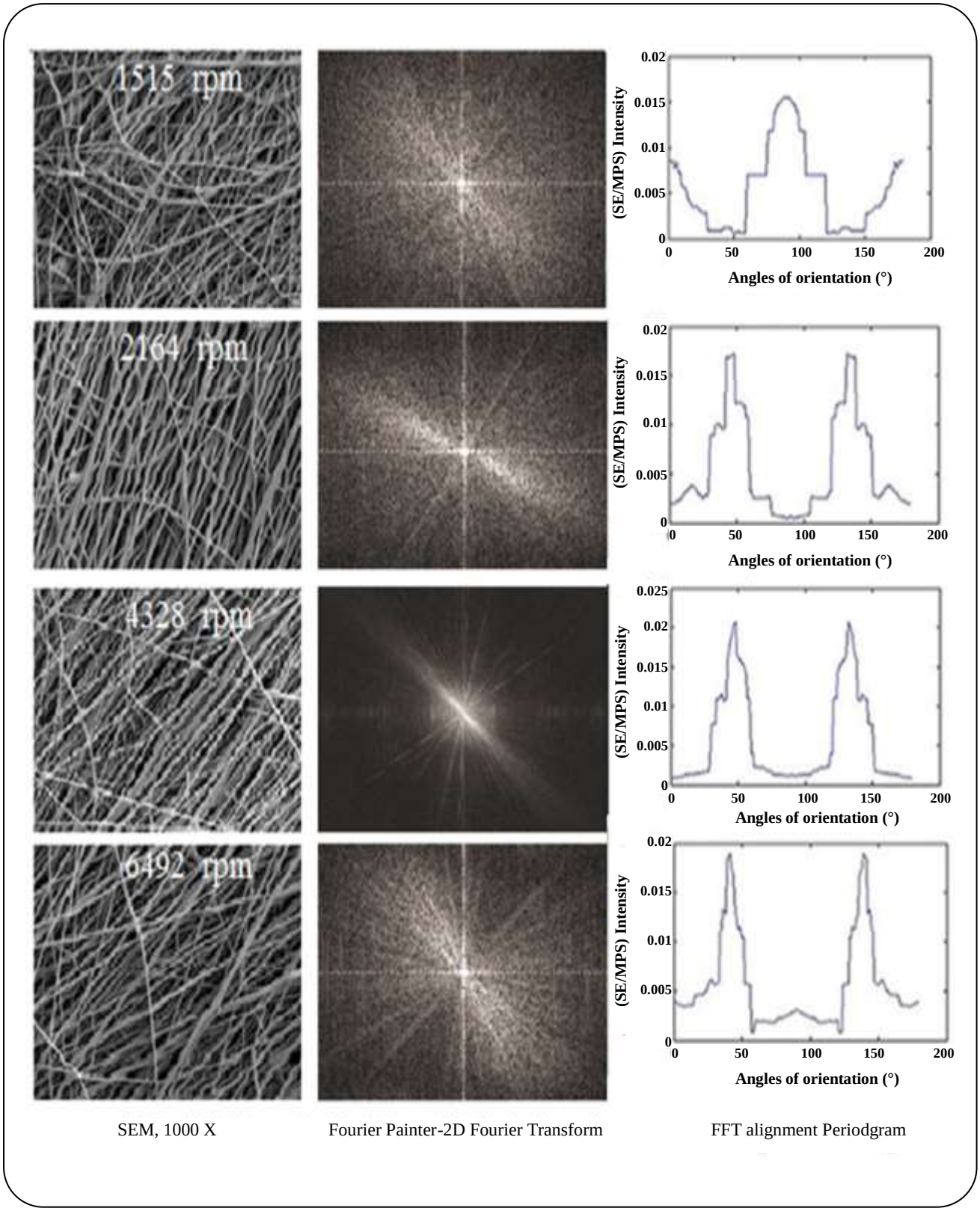

Fig. 10: SEM micrographs, Fourier Painter-2D Fourier Transforms images and the FFT alignment Periodgram of the nanofibers produced from the 15 wt.% polymer solution at four take-up speeds fabricated through opposite charge electrospinning method..

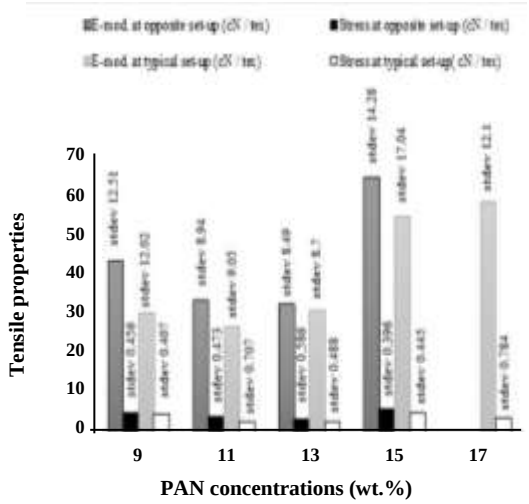

Fig. 11: Plot of Stress and E-mod against polymer concentration for both electrospinning methods.

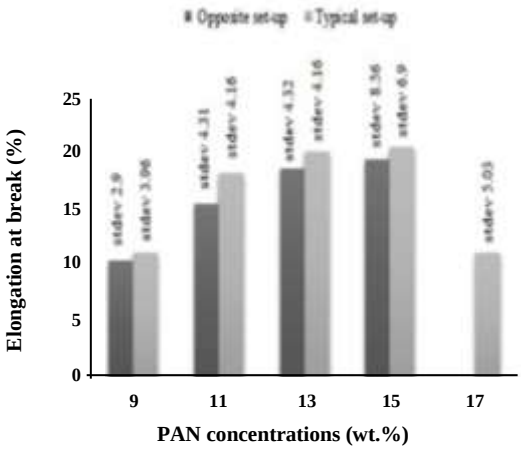

Fig. 12: Elongation at the break as a function of concentration for nanofibers obtained from polymer solutions with different concentrations for both electrospinning methods.

the needle and collector in the typical set-up. However, the nanofibers produced from either method were best aligned at the rotating mandrel speed of 4328 rpm. Also, the linear speed of the rotating mandrel surface surging as a fiber take-up device, matches that of evaporated jet depositions, the fibers are taken up on the surface of the mandrel tightly in a circumferential manner, resulting in a fair alignment. Such a speed is referred to as an alignment speed. If the surface speed of the mandrel is slower than the alignment speed, randomly deposited fibers will be collected. The observed declining of the alignment of nanofibers at the take-up speed of 6492 rpm, can be attributed to the drawing mechanism which inherently uncoils the molecular chain to reach higher orientation, but after an optimum take up speed the braking force acting on the molecular chain starts to build up. At the early stage, the decrease of nanofiber alignment can be observed due to partial segregation of the polymer chains and reform of the coiled structure [34].

Effect of the Electrospinning Parameters on tensile Properties of Nanofibrous tubular structure

These set of experiments were performed on the nanofibers produced from the varying polymer solution concentrations (9, 11, 13, 15 and 17 wt.%) and (9, 11, 13 and 15wt.%) by the typical and opposite charge electrospinning methods respectively while keeping all other electrospinning parameters constant. Tensile samples were prepared according to ASTM D-638-14. Fig. 11 is the plot of Stress and E-modulus against polymer concentration and Fig. 12 presents elongation at the break as a function of polymer solution concentration for nanofibers obtained from both electrospinning methods. Tensile properties enhanced for the nanofibers produced from higher concentrations of polymer solutions. As mentioned earlier, fiber alignment had improved at higher polymer concentrations and the nanofibers resulting from the electrospinning of the 15 wt.% polymer solution through the typical set-up. It was this improvement of directional alignment which lead to improving the tensile properties of the nanofibers as compared with the ones obtained from lower polymer solution concentrations with lower directional nanofiber alignments. It has been stated by various researchers that, orientation of nanofibers is in direct relationship with mechanical properties [21, 35, 36].

To study the effect of take-up speed on tensile properties, the concentration of PAN solution was kept constant as 15wt.%, along with other electrospinning parameters. These electrospinning operating conditions were applied to both the typical and opposite charge set-ups. Figs. 13 and 14 show the stress and elongation at break respectively, for the nanofibers produced from the 15 wt.% polymer solution at the different rotational speed of the mandrel collector for the typical and opposite charge electrospinning methods.

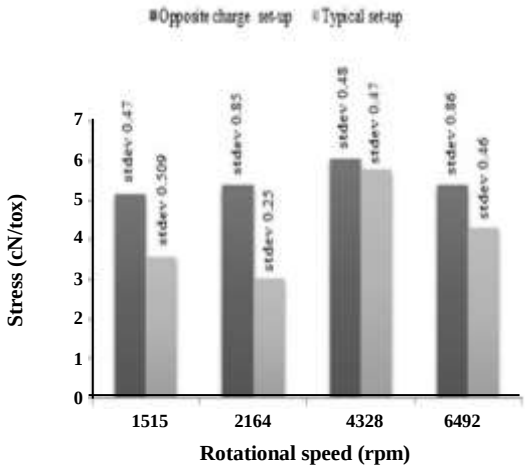

Fig. 13: Tensile stress versus mandrel collector speed for the nanofibers produced from the 15 wt.% polymer solution at a different rotational speed of the mandrel collector for the typical and opposite charge electrospinning methods.

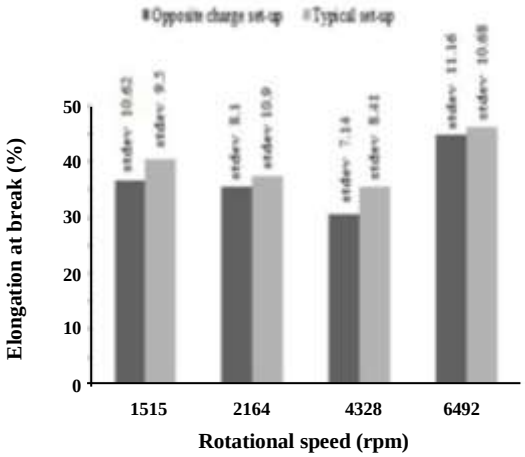

Fig. 14: Elongation at the break as a function of mandrel collector speed for the nanofibers produced from the 15 wt.% polymer solution at different rotational speed of the mandrel collector for the typical and opposite charge electrospinning methods.

The Nano fibrous samples collected at higher rotation speeds, such as 4328 and 6492 rpm showed higher tensile strengths, unlike the ones collected at a rotation speed as low as 1515 rpm. Elongations at break (%) obtained for the nanofibers produced by the typical setup were higher than those obtained from the opposite charge setup at all the take-up speeds, indicating different breaking mechanisms for the randomly oriented and directionally aligned nanofibers. It is mentioned earlier under the heading of the effect of the take-up speed on the alignment of nanofibers that, the nanofibers fabricated through the opposite charge method were more directionally aligned as compared with those prepared by the typical set-up. When subjected to tensile stress, nanofibers oriented in the direction of cross-head displacement were stretched uniaxially, while fibers oriented at some angles with the principal elongation at break direction, experienced a rotation. Eventually, the junctions and adhesion between fibers at various bonding sites were highly distressed before breaking broken. For aligned fibrous structures, the fibers have already been oriented in the direction of displacement and thus, the elongation at break was loaded along fibers themselves, and most fibers were stretched broken. In addition, there was much less fiber rotation compared to non-aligned fibers. *Mo. X.* and *coworkers* [16] explained the observed fundamental difference in the tensile behavior of the two forms of nanofibers through morphological characterization of broken fibers for random and aligned nanofibers. According to the data obtained, an inversion point for the anisotropy of mechanical properties was estimated to be around 2164 rpm. The nanofibers obtained at the take-up speed of 4328 rpm produced by either of the electrospinning methods exhibited the highest tensile strength. The variation of the rotating mandrel collector speed leads to changes in the material mechanical anisotropy index which are defined as the ratio of the mechanical property in the longitudinal direction to that in the circumferential direction [25]. The aspect ratio (length/diameter) of the nanofibers also increased with increasing the take-up speed. Increasing the rotating mandrel collector speed, the mechanical force of stretching (drawing) the jet of the electrospun nanofibers increased, resulting in the formation of nanofibers with smaller diameter, which in turn improved the crystallinity and molecular orientation of the fibers, which explains the enhanced tensile properties for smaller diameter fibers. Many studies have shown a strong correlation between mechanical properties and fiber alignment by using speed collector [24, 25, 37-40].

Effect of the Electrospinning Parameters on Crystalline Properties of Nanofibrous tubular structures

X-rays penetrate into the solid non-destructively and provide information about the inner structure of solids. The crystal acts as a natural diffraction grating for the

diffraction of X-ray beam incident upon it in all directions. The X-rays are diffracted in accordance with the Bragg's law:

$$n\lambda = 2d\sin\theta \quad (2)$$

Where *n* is an integer referring to the order of reflection, λ is the wavelength, *d* is the spacing between the crystal lattice planes responsible for particular diffracted beam and θ is the angle that incident beam makes with lattice planes. The width of the Bragg's reflection in a standard X-ray powder diffraction pattern can provide the information of the average grain size. The peak breadth increases as the grain size decreases, because of the reduction in the coherently diffracting domain size, which can be assumed to be equal to the average crystallite size. The average particle size can be estimated by using Scherer's relation:

$$D = K\lambda/\beta\cos\theta \quad (3)$$

Where λ is the X-ray wavelength, β is the full width at half maximum of diffraction peak, θ is the diffraction angle and *K* is the Scherer's constant of the order of unity for the usual crystal [29, 41, 42]. Where λ=1.54Å and K=0.90, β=FWHM at reflection intensity 100%. The degree of orientation Π (%) can be estimated by using the fully corrected azimuthal intensity distribution diffracted from the (100) reflection at d-spacing [Å]. The degree of orientation can be calculated by the following equation.

$$\Pi = \frac{180^\circ - \Delta\varphi^{1/2}}{180^\circ} \quad (4)$$

Where $\Delta\varphi^{1/2}$ represents the FWHM of the azimuthally scanned peak and the φ represents the corrected (χ) azimuthal angles between the deformation direction and the normal direction of individual crystal planes. This angle can be calculated by the equations [43]:

$$(x) = \theta - \text{FWHM} \quad (5)$$

And

$$\cos\varphi = \cos\chi\cos\theta \quad (6)$$

Crystallinity (%) and the crystallite size (nm) of the nanofibrous tubular structures was examined XRD at room temperature. Crystallinity is commonly measured as a ratio of the diffraction portion from the crystalline part of the sample (Ic), and the total diffraction from the same sample ($I=I_C + Ib$). The values of Ic can be obtained after an appropriate subtraction of the scattering portion from the background (Ib).

$$C\% = \frac{I_C}{I}100\% \quad (7)$$

where , C% was crystallinity (%) [44, 45]. In the X'Pert Pro system, the calculation of crystallinity (%) was done by the user defined crystalline (peak area) and amorphous regions (background area) on a frame obtained from the analyzed material. The software integrated all pixels within the "peak area" as well as all pixels within the "background area" in order to obtain the values for Ic + Ib in the above equation. The background in these measurements was calculated as a 2_{nd} order polynomial by least squares method and was automatically subtracted from the total intensity of the "peak area" in order to obtain Ic. The "peak area" and the "background area" were kept constant for all samples. The experimental results so far proved the rotating mandrel collector speed as one of the most important electrospinning parameters affecting the properties of the fabricated nanofibers, including tensile properties. All the electrospinning parameters except the rotating mandrel collector speed were kept constant for both the typical and opposite charge methods used to produce nanofibers (from 15 wt.% polymer solution) in this set of experiments. Figs. 15 and 16 show the XRD pattern for the nanofibers produced at four different rotating mandrel speeds by the typical and the opposite charge electrospinning methods, respectively. And Fig. 17 well compares the degree of orientation (%), crystallite size (nm) and crystallinity (%) of the nanofibers produced by typical and opposite charge methods at four different take-up speeds. The results obtained from the XRD experiments indicated that crystallinity (%), crystallite size (nm) and degree of orientation (%) of the nanofibers were all enhanced as the rotating mandrel collector speed increased, being more pronounced for the nanofibers produced by the opposite charge method. Also, FWHM decreased due to increasing degree of orientation, crystallite size, and crystallinity as the fibers were stretched and aligned toward the roll-up direction together with control on the diameter of the fiber via drawing. Thus, it can be figured out as how

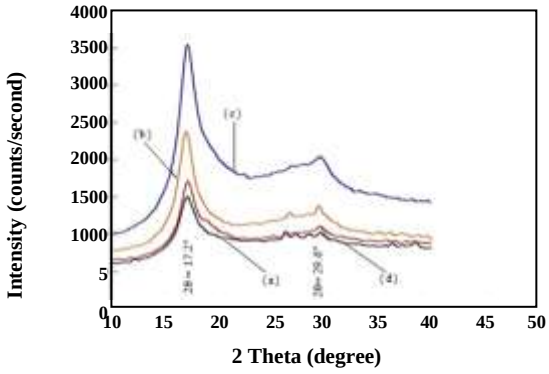

Fig. 15: XRD pattern of the nanofibers produced at four different take-up speeds by the typical set-up, where: a, b, c, and d correspond to the rotating mandrel speeds of 1515, 2164, 4328 and 6492 rpm, respectively.

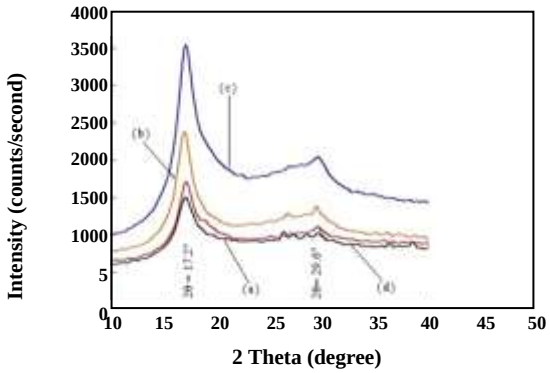

Fig. 16: XRD pattern of the nanofibers produced at four different take-up speeds by the opposite charge setup, where: a, b, c, and d correspond to the rotating mandrel speeds of 1515, 2164, 4328 and 6492 rpm, respectively.

the electrospinning process, as well as the mechanical drawing, affected the crystal morphology and molecular orientation of nanofibers. The best results were exhibited by the samples obtained at the take-up speed of 4328 rpm produced by either of the electrospinning methods. Variation of the rotating mandrel speed resulted in changing the mechanical anisotropy index [46]. The increase in the number of crystalline regions increased the rigidity of the nanofibrous structures. Samples obtained by both the electrospinning methods produced a main strong XRD peak at $2\theta = 17.2°$ and a weak one at $2\theta = 29.6°$. This behavior confirmed that crystallization was retarded during the electrospinning process, which could be attributed to the rapid solidification of the stretched polymeric chains at high elongation rates during the later stages of electrospinning that significantly hindered the formation of crystals. In other words, the polymer chains did not have enough time to organize into 3D ordered crystal structures before they were solidified. Thus, higher crystallinity in the fibers was associated with the higher tensile strength of the fibers, which has also been observed by other researchers [9, 44].

CONCLUSIONS

Polyacrylonitrile nanofibrous tubular strictures were fabricated by typical and opposite charge electrospinning methods. Increasing polymer solution concentration considerably increased the diameter of the nanofibers produced through both electrospinning methods, however, the increasing ranges of the average diameters were larger for the nanofibers produced by the opposite charge set-up. Fewer beads were formed along the length of the nanofibers (more uniform fibers were formed) as the polymer solution concentration increased and also the bead shapes were changed from spherical to spindle-like, the number, and size of which were smaller for those produced by the opposite charge method. The best performing PAN electrospinning solution concentration was 15 wt.% among the four solutions studied by both the electrospinning set-ups. Nanofibers diameter decreased as the speed of the rotational mandrel increased and the observed decline was greater in the opposite charge method, especially at higher concentrations of polymer solution. A higher concentration of PAN solutions, as well as higher take-up speeds, also resulted in higher alignment of nanofibers, being more pronounced for the opposite charge method and the optimum alignment speed obtained for both the electrospinning methods was 4328 rpm. Tensile properties were enhanced for the nanofibers produced from higher concentrations of polymer solutions as well as higher take-up speeds, as they had higher directional alignment, however, different breaking mechanisms for the randomly oriented fibers and directionally aligned nanofibers were observed. An inversion point for the anisotropy of mechanical properties was found to be around 2164 rpm. Crystallinity (%), crystallite size (nm) and degree of orientation (%) of the nanofibers were all enhanced as the rotating mandrel collector speed increased, being more pronounced for the nanofibers produced by the opposite charge method.

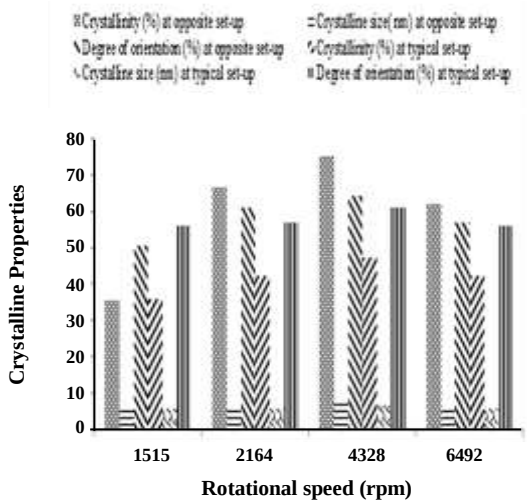

Fig. 17: The degree of orientation (%), the crystallite size (nm) and crystallinity (%) of the nanofibers produced by typical and opposite charge methods at four different take-up speeds.

Nomenclatures

D	Crystalline size, nm
C	Percentage of crystallinity, %
stdev	Standard deviation of average nanofibers diameter, nm
d	Distance between needle and collector, cm
S	Solution feed rate, mL/h
R	Rotational speed of collector, rpm
A	Applied voltage, kV
Co	Concentration of PAN in DMF, wt. %
D	Distance between two needles, cm
Π	Percentage of degree orientation, %
Å	Physical unit for measuring the Spacing between the crystal lattice planes, 0.1 nm
θ	Angle that incident beam makes with lattice planes, 0-∏
β	Width of the Bragg's reflection
K	Scherer's Constant
FWHM	Full width at half maximum of diffraction peak
Π	Percentage of degree of orientation
$\Delta\varphi^{1/2}$	FWHM of the azimuthally scanned peak
Λ	X-ray wavelength, λ = 1.542 Å
χ	Azimuthal Angles
φ	Corrected Azimuthal Angles

Received : Dec. 3, 2017 ; Accepted : Apr. 23, 2018

REFERENCES

[1] Mohammad M.A., Sara A., Hossein F., Enhanced Ferroelectric Properties of Electrospun Poly(vinylidene fluoride) Nanofibers by Adjusting Processing Parameters, *RSC Adv.*, **5**: 61277 -61283 (2015) .

[2] Homaeigohar S., Elbahri M., Nanocomposite Electrospun Nanofiber Membranes for Environmental Remediation, *Materials*, **7**(2): 1017-1045 (2014).

[3] Ganjkhanlou Y., Bayandori Moghaddam A., Hosseini S., Nazari T., Gazmeh A., Badraghi J., Application of Image Analysis in the Characterization of Electrospun Nanofibers, *Iran. J. Chem. Chem. Eng.(IJCCE)*, **33**: 37-45 (2014).

[4] Almasi, D., Abbasi, K., Sultana, N., Lau, W., Study on TiO_2 Nanoparticles Distribution in Electrospun Polysulfone/TiO2 Composite Nanofiber, *Iran. J. Chem. Chem. Eng.(IJCCE)*, **36**(2): 49-53 (2017).

[5] Dabirian F., Hosseini S., Novel Method for Nanofibre Yarn Production Using Two Differently Charged Nozzles, *Fibres Text. East. Eur.*, **17**(3): 45-47 (2009).

[6] Chen J., Niu Q., Chen G., Nie J., Ma G., Electrooxidation of Methanol on Pt@ Ni Bimetallic Catalyst Supported on Porous Carbon Nan fibers, *J. Phys. Chem. C* , **121**(3): 1463-1471 (2017)

[7] Shi Q., Lei Y., Wang Y., Wang H., Jiang L., Yuan H., Gou Y.B, N-codoped 3D Micro-/Mesoporous Carbon Nanofibers Web as Efficient Metal-free Catalysts for Oxygen Reduction. Current, *J. Appl. Phys.*, **15**(12): 1606-1614 (2015).

[8] Xie J., MacEwan M.R., Schwartz A.G., Xia Y., Electrospun Nanofibers for Neural Tissue Engineering, *Nanoscale*, **2**(1): 35-44 (2010).

[9] Mottaghitalab V., Haghi A.K., A Study on Electrospinning of Polyacrylonitrile Nanofibers, *Korean J. Chem. Eng .*,**28**(1):114-118(2011).

[10] Panda P, Ceramic Nanofibers by Electrospinning Technique—A Review. Trans, *Indian Ceram. Soc.*, **66**(2):65-76 (2007).

[11] Yener F., Jirsak O., Gemci R., Using a Range of PVB Spinning Solution to Acquire Diverse Morphology for Electrospun Nanofibres, *Iran. J. Chem. Chem. Eng. (IJCCE)*, **31**(4): 49-58 (2012).

[12] Beachley V., Wen X., Effect of Electrospinning Parameters on the Nanofiber Diameter and Length, *Mater. Sci. Eng. C*, **29**(3): 663-668 (2009).

[13] Garg K , Bowlin G.L., Electrospinning Jets and Nanofibrous Structures, *Biomicrofluidics*, **5**(1): 013403 (2011).

[14] Huang Z.M., Zhang Y.Z., Kotaki M., Ramakrishna S., A Review on Polymer Nan Ofibers by Electrospinning and Their Applications in Nanocomposites, *Compos. Sci. Technol.*, **63**(15): 2223-2253 (2003).

[15] Bhardwaj N., Kundu S.C., Electrospinning: A Fascinating Fiber Fabrication Technique, *Biotechnol. Adv.*, **28**(3): 325-347 (2010).

[16] Mo X., Xu C., Kotaki M., Ramakrishna S., Electrospun P (LLA-CL) Nanofiber: A Biomimetic Extracellular Matrix for Smooth Muscle Cell and Endothelial Cell Proliferation, *Biomaterials*, **25**(10): 1883-1890 (2004).

[17] Yang F., Xu C., Kotaki M., Wang S., Ramakrishna S., Characterization of Neural Stem Cells on Electrospun Poly (L-lactic acid) Nanofibrous Scaffold, *J. Biomater. Sci., Polym. Ed*, **15**(12): 1483-1497 (2004).

[18] Sreedhara S.S., Tata N.R., A Novel Method for Measurement of Porosity in Nanofiber Mat Using Pycnometer in Filtration, *J Eng Fiber Fabr.*, **8**(4): 132-137 (2013).

[19] Niu H., Wang X., Lin T., "Needleless electrospinning: Developments and Performances. InNanofibers-Production, Properties and Functional Applications", InTech,(2011).

[20] Chen M., Patra P.K., Warner S.B., Bhowmick S., Optimization of Electrospinning Process Parameters for Tissue Engineering Scaffolds, *Biophys ,Rev. Lett.*, **1**(2): 153-178 (2006).

[21] Wu H., Fan J., Chu C.C., Wu J., Electrospinning of Small Diameter 3-D Nanofibrous Tubular Scaffolds with Controllable Nanofiber Orientations for Vascular Grafts, *J Mater Sci Mater Med.*, **21**(12): 3207-3215 (2010).

[22] Fennessey S.F., Farris R.J., Fabrication of Aligned and Molecularly Oriented Electrospun Polyacrylonitrile Nanofibers and the Mechanical Behavior of Their Twisted Yarns, *Polymer* ,**45**(12): 4217-4225 (2004).

[23] Sadrjahani M., Hoseini S. , Mottaghitalab V. , Haghi A., Development and Characterization of Highly Oriented Pan Nanofiber, *Braz. J. Chem. Eng.*, **27**(4): 583-589 (2010).

[24] Kenawy E.R., Layman J.M., Watkins J.R., Bowlin G.L., Matthews J.A., Simpson D.G., Wnek G.E., Electrospinning of Poly (ethylene-co-vinyl alcohol) Fibers, *Biomaterials*, **24**(6): 907-913 (2003).

[25] Bonani W., Maniglio D., Motta A., Tan W., Migliaresi C., Biohybrid Nanofiber Constructs with Anisotropic Biomechanical Properties., *J Biomed Mater Res B Appl Biomater*, **96**(2): 276-286 (2011).

[26] Enis I.Y., Sezgin H., Sadikoglu T.G., Full Factorial Experimental Design for Mechanical Properties of Electrospun Vascular Grafts, *J. Ind. Text.*, (2017).

[27] Yalcin Enis I., Horakova J., Gok Sadikoglu T., Novak O., Lukas D., Mechanical Investigation of Bilayer Vascular Grafts Electrospun from Aliphatic Polyesters, *Polym. Adv. Technol.*, **28**: 201–213 (2017).

[28] Kurban Z., Lovell A., Jenkins D., Bennington S., Loader I., Schober A., Skipper N., Turbostratic Graphite Nanofibres from Electrospun Solutions of PAN in Dimethylsulphoxide, *Eur. Polym. J.*, **46**(6): 1194-1202 (2010).

[29] Cao G., "Nanostructures and Nanomaterials: Synthesis, Properties and Applications", World Scientific , Imperial College Press, (2004).

[30] Jalili R., Morshed M., Ravandi S.A., Fundamental Parameters Affecting Electrospinning of PAN Nanofibers as Uniaxially Aligned Fibers, *J. Appl. Polym. Sci.*,**101**(6): 4350-4357 (2006).

[31] Stokols S., Tuszynski M.H., Freeze-Dried Agarose Scaffolds with Uniaxial Channels Stimulate and Guide Linear Axonal Growth Following Spinal Cord Injury, *Biomaterials*, **27**(3): 443-451 (2006).

[32] Teo W.E., Kotaki M., Mo X.M., Ramakrishna S. , Porous Tubular Structures with Controlled Fibre Orientation Using a Modified Electrospinning Method, *Nanotechnology*, **16**(6): 918 (2005).

[33] Kim J.I., Hwang T.I., Aguilar L.E., Park C.H., Kim C.S., A Controlled Design of Aligned and Random Nanofibers for 3D bi-Functionalized Nerve Conduits Fabricated via a Novel Electrospinning Set-up, *Scientific Reports*, **6**: 23761- (2016).

[34] Khamforoush M., Asgari T., Hatami T., Dabirian F., The Influences of Collector Diameter, Spinneret Rotational Speed, Voltage, and Polymer Concentration on the Degree of Nanofibers Alignment Generated by Electrocentrifugal Spinning Method: Modeling and Optimization by Response Surface Methodology, *Korean J. Chem. Eng.*, **31**(9): 1695-1706 (2014).

[35] Aljehani A.K., Hussaini M.A., Hussain M.A., Alothmany N.S., Aldhaheri R.W., "Effect of Electrospinning Parameters on Nanofiber Diameter Made of Poly (vinyl alcohol) as Determined by Atomic Force Microscopy", *In: Biomedical Engineering (MECBME), Middle East Conference* on 2014 Feb 17 (pp. 379-381). IEEE, (2014).

[36] Zhou Z., Lai C., Zhang L., Qian Y., Hou H., Reneker D.H., Fong H. , Development of Carbon Nanofibers from Aligned Electrospun Polyacrylonitrile Nanofiber Bundles and Characterization of Their Microstructural, Electrical, and Mechanical Prope, *Polymer* ,**50**(13): 2999-3006 (2009).

[37] Li W.J., Mauck R.L., Cooper J.A., Yuan X., Tuan R.S., Engineering Controllable Anisotropy in Electrospun Biodegradable Nanofibrous Scaffolds for Musculoskeletal Tissue Engineering, *J. Biomech.*, **40**(8): 1686-1693 (2007).

[38] Pan Z.J., Liu H.B., Wan Q.H ., Morphology and Mechanical Property of Electrospun PA 6/66 Copolymer Filament Constructed of Nan Fibers, *Journal of Fiber Bioengineering and Informatics (JFBI)*, **1**(1): 47-54 (2008).

[39] Fornes T.D., Paul D.R., Formation and Properties of Nylon 6 Nanocomposites, *Polímeros*, **13**(4): 212-217 (2003).

[40] Wong S.C., Baji A., Leng S., Effect of Fiber Diameter on Tensile Properties of Electrospun Poly (ε-caprolactone), *Polymer*, **49**(21): 4713-4722 (2008).

[41] Azarkhalil M.S, Keyvani B. Synthesis of Silver Nanoparticles from Spent X-Ray Photographic Solution via Chemical Rreduction. *Iran. J. Chem. Chem. Eng. (IJCCE)*, **35**(3): 1-8 (2016).

[42] Cullity B.D., "Diffraction 1: The Directions of Diffracted Beams. Elements of X-Ray Diffraction", Addison-Wesley Publishing Co., Inc., USA, (1956).

[43] Zhang Y., Leblanc-Boily V., Zhao Y., Prud'homme R.E.,Wide Angle X-Ray Diffraction Investigation of Crystal Orientation in Miscible Blend of Poly (ε-caprolactone)/poly (vinyl chloride) Crystallized under Strain, *Polymer*, **46**(19): 8141-8150 (2005).

[44] Alemdar A., Sain M., Isolation and Characterization of Nanofibers from Agricultural Residues–Wheat Straw and Soy Hulls, Bioresour, *Technol*., **99**(6): 1664-1671 (2008).

[45] Song Z., Hou X., Zhang L., Wu S., Enhancing Crystallinity and Orientation by Hot-Stretching to Improve the Mechanical Properties of Electrospun Partially Aligned Polyacrylonitrile (PAN) Nanocomposites, *Materials* , **4**(4): 621-632 (2011).

[46] Mai F., Tu W., Bilotti E., Peijs T., The influence of Solid-State Drawing on Mechanical Properties and Hydrolytic Degradation of Melt-Spun Poly (lactic acid)(PLA) Tapes., *Fibers*, **3**(4): 523-538 (2015).